Appendix 1

Probability of EPR-Generated Hydrogen Bond Arrangements, *keto-amino → enol-imine*, Using Approximate Quantum Methods [50]

Natural selection has designed duplex genomes for the time-dependent populating of initially unoccupied, but energetically accessible, enol and imine entangled proton qubit states [35-39] as consequences of quantum uncertainty limits [2,66], $\Delta x \, \Delta p_x \geq \hbar /2$, operating on metastable amino ($-NH_2$) hydrogen bonding protons [15-23,54,65]. The resulting quantum confinement introduces direct quantum mechanical proton – proton physical interaction into too small of space, Δx, thereby generating probabilities of EPR arrangements, *keto-amino → enol-imine,* which create position and momentum entanglement between separating product protons [29-31,35-39].

Each reduced energy product proton is shared between two indistinguishable sets of electron lone-pairs belonging to enol oxygen and imine nitrogen, and thus, participates in entangled quantum oscillations at ~ 4×10^{13} s^{-1} between near symmetric energy wells within intramolecular decoherence-free subspaces [35-39,67-69], until "measured by" [11,42-45] Grover's-type [40] enzyme quantum processors [35-39]. In intervals $\delta t << 10^{-13}$ s, the quantum reader "traps" an entangled oscillating qubit, H$^+$, in a DNA groove [70]. This creates an enzyme – proton entanglement that instantaneously specifies explicit instructions for an entangled enzyme quantum search, $\Delta t' \leq 10^{-14}$ s [13,36], to select the correct incoming tautomer for pairing with the ultimately decohered eigenstate [14,35-39], which forms the observable molecular clock substitution, *ts* [15-22,37-38]. Since specification of the molecular clock, *ts* or *td,* is completed before proton decoherence, $\Delta t' < \tau_D < 10^{-13}$ s [13], a feedback loop exists between an entangled enzyme quantum processor "measurement" and initiation of duplex genome evolution [35-39].

For purposes of discussing metastable keto-amino states populating reduced energy enol and imine, dynamic entangled proton qubit states, G-C → *G'-C'* and G-C → **G-*C*, time- dependence for the reactive five proton system of metastable G-C to populate complementary entangled proton qubit states is modeled in terms of a "composite" proton, in an asymmetric three-well potential [98], illustrated in Figure 19. An expression is obtained for the quantum mechanical "rate constant" associated with the EPR hydrogen bond arrangement, *keto-amino → enol-imine,* via symmetric and asymmetric channels (Figures 2,3; Table 2). This allows development of a polynomial expression for an evolving Darwinian, genomic system to express time-dependent alterations classical + entanglement originated in genetic specificities at DNA base pairs within a specified gene [35-39,54,104].
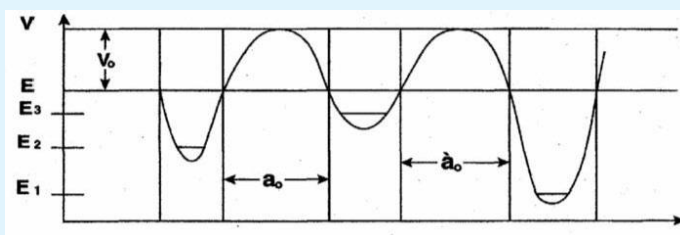

Figure 19: Qualitative energy surface for a composite DNA proton system occupying the metastable, hybrid and ground states.
(Figure 19 Asymmetric three-well potential to simulate meta stable keto-amino protons populating accessible enol-imine states in terms of a "composite" proton originating in the meta stable E_3 energy well at t = 0 where $E_1 < E_2 < E_3$).

Here the motion of two tunneling-exchange protons, using the symmetric and asymmetric channels (Figure 2-3), is simulated in terms of a composite proton model. Secondary contributions by the 2nd asymmetric pathway (unlabeled) are neglected. At t = 0, the composite proton is replicated into the meta stable state ⎪3 > at energy E_3 which, per data [20-21] and shown in Figure 19, is separated from the enol-imine ground state, ⎪1>, and hybrid state, ⎪2>, by approximately equal energy barriers. The relationship $E_1 < E_2 < E_3$ for the ground state, hybrid state and meta stable state, respectively, is

displayed in Figure 19. Enol-imine product states are designated by a general arrangement state, $|\rho>$, where the energy E_ρ would equal E_1 or E_2 as appropriate. Time-dependence of an eigenstate, $|\Psi>$, is expressed by $|\Psi>=|\varphi_I> \exp(-i\, E_i\, t/\hbar)$, so $|\Psi>=|\varphi_I>$ at t = 0 [2]. The relationship $|\Psi>=\sum_i |i><i|\Psi>$ is used to express an eigenstate $|\Psi>$ in terms of base states $|i>$ and amplitudes C_i as

$$|\Psi>=|1><1|\Psi>+|2><2|\Psi>=|1>C_1+|2>C_2 \quad (25)$$

where base states satisfy $<i\,|\,j>=\delta_{i\,j}$. The eigenstate is normalized, $<\Psi|\Psi>=1$, and an eigenstate and eigen value E are related to the Hamiltonian matrix, $\sum_{ij}<i|H|j>$, by $\sum_j<i|H|j><j|\Psi>=E<i|\Psi>$, which can be rewritten as

$$\sum_j (H_{ij}-E^k\delta_{ij})C^k_{\ j}=0 \quad (26)$$

for an expression to solve for amplitudes, $\{C^k_j |_{\ i=1,2;\ j=1,2}\}$. A nonzero solution to Equation (26) is available if the determinant of $\sum_j (H_{ij}-E\delta_{ij})=0$.

A two-level Hamiltonian that will allow a composite proton to tunnel from the metastable state $|3>$ at energy E_3, to an arrangement state $|\rho>$ at energy E_ρ, can be written as

$$H=\begin{pmatrix} E_3 & -\alpha_\rho \\ -\alpha_\rho & E_\rho \end{pmatrix}=\begin{pmatrix} H_{11} & H_{12} \\ H_{21} & H_{22} \end{pmatrix}$$

where α_ρ is the quantum mechanical coupling between states $|3>$ and $|\rho>$. The resulting upper and lower eigenvalues, $E_{A\rho}$ and $E_{B\rho}$, are found as

$$E_{A\rho}=\xi_\rho+\gamma_\rho \quad (28)$$

and
$$E_{B\rho}=\xi_\rho-\gamma_\rho \quad (29)$$

where $\xi_\rho = (E_3 + E_\rho)/2$, $\gamma_\rho = [(E_3 - E_\rho)^2/4 + \alpha_\rho^2]^{1/2}$ and ρ = 1, 2 for the symmetric and asymmetric channels, respectively. The time-dependent wave function, $|\Psi(t)>$, of the composite proton in the asymmetric three-well potential can be expressed in terms of the corresponding eigen states as

$$|\Psi|\Psi(t)>=|\Psi_{A1}>\exp(-iE_{A1}\,t/\hbar)+|\Psi_{A2}>\exp(-iE_{A2}\,t/\hbar)$$
$$+|\Psi_{B1}>\exp(-i\,E_{B1}\,t/\hbar)+|\Psi_{B2}>\exp(-iE_{B2}\,t/\hbar) \quad (30)$$

which can be expressed in terms of physical base states
$$|3>,\ |2>,\ |1> \text{ as [183] (31)}$$

$$|\Psi(t)> = \exp(-i\,\xi_1\,t/\hbar)\{|3> \exp(-i\,\gamma_1\,t/\hbar) + |1'> \exp[-i(\gamma_1\,t/\hbar+\delta)]\}$$
$$+\exp(-i\,\xi_1\,t/\hbar)\{|3> \exp(+i\,\gamma_1\,t/\hbar) + |1'> \exp[+i(\gamma_1\,t/\hbar+\delta)]\}$$
$$+\exp(-i\,\xi_2\,t/\hbar)\{|3> \exp(-i\,\gamma_2\,t/\hbar) + |2'> \exp[-i(\gamma_2\,t/\hbar+\delta)]\}$$
$$+\exp(-i\,\xi_2\,t/\hbar)\{|3> \exp(+i\,\gamma_2\,t/\hbar) + |2'> \exp[+i(\gamma_2\,t/\hbar+\delta)]\}$$

This can be written more succinctly as

$$|\Psi(t)> = (0.5)^{\frac{1}{2}}\exp(-i\xi_1\,t/\hbar)\{|3> \cos(\gamma_1\,t/\hbar) + |1'> \sin(\gamma_1\,t/\hbar)\}$$
$$+(0.5)^{\frac{1}{2}}\exp(-i\xi_2\,t/\hbar)\{|3> \cos(\gamma_2\,t/\hbar) + |2'> \sin(\gamma_2\,t/\hbar)\} \quad (32)$$

where $|1> = |1'>e^{i\,\delta}$, $|2> = |2'>e^{i\,\delta}$ and δ of the arbitrary phase factor $e^{i\,\delta}$ is $-\pi/2$ and the relation $\cos(\theta - \pi/2) = \sin(\theta)$ is used. Data show that *ts* rates are approximately equal for transversions and transitions [20-21]; so, quantum mechanical "rate constants" for EPR arrangements, *keto-amino → enol-imine* via symmetric and asymmetric channels, are approximately equal (Figure 19). Since the lifetimes, τ, for 37⁰C keto-amino G-C protons are, $\tau \geq 3{,}000$ years (Table 5) [50], the wave function expression in Equation (32) would be applicable in the interval, $0 < t < 3{,}000$ years.

At t = 0, the composite proton was in the meta stable state $|3>$ at energy E_3. The probability, $P_1(t)$, that the proton is in the ground state $|1>$ at later time, t, is given by

$$P_1(t) = |<1'|\Psi(t)>|^2 = 0.5\sin^2(\gamma_1\,t/\hbar) \quad (33)$$

which identifies $P_1(t)$ in terms of contributions by the symmetric channel. The probability of the proton being in the hybrid state $|2>$ later is given as

$$P_2(t) = |<2'|\Psi(t)>|^2 = 0.5\sin^2(\gamma_1\,t/\hbar) \quad (34)$$

which is the contribution by the asymmetric channel. The probability that the proton is in meta stable state $|3>$ at time t is given by

$$P_3(t) = |<3'|\Psi(t)>|^2 = 0.5\left[\cos^2(\gamma_1\,t/\hbar) + \cos^2(\gamma_2\,t/\hbar)\right] \quad (35)$$

which is the sum of contributions for protons existing state $|3>$ by the symmetric and asymmetric channels. The sum of Equations (33 to 35), given by

$$\sum_{i=1}^{3}P_i(t) = (0.5)\left[\sin^2\left(\frac{r_1 t}{\hbar}\right) + \cos^2\left(\frac{r_1 t}{\hbar}\right)\right] + (0.5)\left[\sin^2\left(\frac{r_2 t}{\hbar}\right) + \cos^2\left(\frac{r_2 t}{\hbar}\right)\right] = 1 \quad (36)$$

is consistent with the requirement that the composite proton be confined to its set of base states, $|3>$, $|2>$, $|1>$. The time derivative of $P_\rho(t)$, Equations (33&34), can be expressed as

$$dP_\rho/dt = (\gamma_\rho/\hbar)\sin(\gamma_\rho\,t/\hbar)\cos(\gamma_\rho\,t/\hbar) \quad (37)$$

where $P_\rho(t)$ represents either $P_1(t)$ or $P_2(t)$ and the 0.5 normalization factor is omitted. A Taylor series expansion of Equation (37) is given by

$$dP_\rho/dt \approx \left(\gamma_\rho/\hbar\right)^2 t - 4/3\left(\gamma_\rho/\hbar\right)^4 t^3 + 4/15\left(\gamma_\rho/\hbar\right)^6 t^5 + \dots \text{ (38)}$$

where the first three terms are given. The experimental lifetime of metastable keto-amino G-C protons is the order of ~3,000 years, which is large compared to human lifetimes of, say, ~100 years. For times t << 3,000 years (e.g., t ≤ 100 years), one could employ a small t approximation to express the probability of metastable protons populating enol and imine states │1 > or │2 > as

$$P_\rho\left(t\right) = \frac{1}{2}\left(\gamma_\rho/\hbar\right)^2 t^2 \text{ (39)}$$

indicating nonlinear time dependence. Nonlinearity of Eq (39) is consistent with exponential increases observed in base substitutions, *ts*, and deletions, *td*, as a function of age in nonmitotic human mt DNA [184]. Equation (39) provides the approximate quantum entanglement term for "biological noise" in Eq (18), and expresses observable quantum contributions in the EPR-entanglement Darwinian polynomial, $\Sigma_j\beta_j t^4$ in Equation (22).

For times t ≤ 100 y, this approximation accounts for the time-dependent contribution of quantum informational content embodied within entangled proton qubits populating decoherence-free subspaces [11,35-39,67-69] of *G'-C', *G-*C* and *A-*T* sites in duplex genomic systems [54,104]. Subsequent enzyme – proton entanglement processing *of* entangled proton qubits introduces entanglement originated "*stochastic*" mutations [100-104], *ts* and *td*, which are expressed in terms of $\Sigma_j\beta_j t^4$ in the EPR-entanglement Darwinian polynomial, Equation (22). Curiously, incidence of age-related (10 to 80 y) human cancer [56] exhibits an empirical ~ t^4 time-dependence (Figure 15), implying phenotypic expression of age-related cancer is a consequence of the quantum entanglement algorithm, yielding decohered product, *ts* and *td*. Based on observation [56] and the model [35,37-39], the EPR-generated quantum entanglement algorithmgenerates SNPs [49-50,100-102], which are expressed as cancer causing "driver" mutations [55,140-143] *after* CNGS, *s* (1 ≥ *s* ≥ 0.97), have been populated by entangled proton qubits to an "unsafe" threshold, i.e., to s ≈ 0.97 + ε. In this case, classical "ball-and-rod" Newtonian mechanisms [27-28,43,115,139] do *not* contribute to "driver" mutation spectra [55,75] for age-related incidence of cancer exhibited in Figure 15.

Appendix 2

Qualitative Calculations on Entangled Proton Qubits

Entangled Proton Qubits via Quantum Uncertainty Limits, Yielding EPR Arrangements, keto-amino → enol-imine

Double helical DNA replicates complementary G-C and A-T base pairs where interstrand keto-amino hydrogen bonds [28,65] are preferable in aqueous environments, but are metastable in unperturbed duplex DNA genomes since reduced energy enol and imine proton qubit states are unoccupied [16-17,35], but energetically accessible via EPR isomerization [29-31,36-39]. The two-metastable hydrogen bonding amino (–NH$_2$) protons are localized on the amino nitrogen (Figures.1-3), and thus, are confined to a relatively small space, Δx, compared to enol and imine entangled proton qubits (Figure 2). The uncertainty relation, Δx Δp$_x$ ≥ ½ ℏ, expresses the product of uncertainties, Δx and Δp$_x$, introduced by quantum confinement effects in any attempt at a simultaneous specification of a position x and corresponding momentum p$_x$ of a particle. In the approximation that p ≈ ℏ/Δx, proton kinetic energy may be approximated by mv^2/2 = p^2/2m = ℏ^2/[2m (Δx)^2].

This illustrates how quantum uncertainty limits on the two amino (–NH$_2$) genome protons can increase proton momentum and kinetic energy, which can cause direct proton – proton physical interaction, leading to probabilities of EPR arrangements, *keto-amino → enol-imine,* where position – momentum entanglement is introduced between

separating product protons [29-31]. Enhanced proton energy could be dissipated through collisional de-excitations, thereby increasing the energy density of "local" chemical bonds in DNA. More energetic vibrational modes would introduce smaller a_0 $V_0^{1/2}$ values in Eq (42).This would increase EPR rates, *keto-amino → enol-imine*, and reduce lifetimes, τ , for meta stable protons. Compared to meta stable hydrogen bonded amino DNA protons, entangled enol and imine product proton qubits oscillate back and forth over larger Δx without possibility of proton-proton interaction causing proton confinement, implying deeper energy wells for reduced energy entangled proton qubits (Figure 19). Each reduced energy product proton is shared between two indistinguishable sets of electron lone-pairs belonging to enol oxygen and imine nitrogen on opposite strands, and thus, participates in entangled quantum oscillations [17,35-39,49-50,54] at ~ 4×10^{13} s^{-1} between near symmetric energy wells in decoherence-free subspaces [67-69]. This specifies quantum dynamics of unperturbed entangled proton qubits until "measured by", $\delta t \ll 10^{-13}$ s, an enzyme quantum reader [35-40,42-45].

Based on molecular genetics observations [15-17,20-21,23], the symmetric channel (Figure 2a) generates time-dependent transversions – $G' → T$&$G' → C$ – but time-dependent transitions – $*C → T$&$*G → A$ – originate via the asymmetric channel (Figure 2b). The *keto-amino* hydrogen bond has two protons "localized" on the amino ($-NH_2$) nitrogen, but "local" protons are absent from the two sets of electron lone-pairs belonging to *keto* oxygen on the opposite strand. A redistribution of the two amino protons over the four sets of electron lone-pairs, plus an appropriate intramolecular redistribution of π and σ electrons [15-17] illustrated in Figure 2, would create a "relaxed" enol – imine hydrogen bond. However, in the case of EPR-generated proton qubit-pairs shared between two indistinguishable sets of electron lone-pairs, each proton qubit will exhibit entangled quantum oscillations between the two near-symmetric energy wells, until "measured by" a Grover's-type "quantum reader" [40].

The asymmetric EPR channel is instigated by quantum uncertainty limits, Δx $\Delta p_x \geq \frac{1}{2}$ ℏ, operating on amino ($-NH_2$) protons of carbon–6 cytosine, which introduces the EPR arrangement, *keto-amino → enol-imine* (Figure 2b), where position – momentum entanglement is introduced between separating enol and imine protons. Proton arrival at guanine carbon-6 keto induces proton transfer at the ring nitrogen position, from G to C, which facilitates a double bond shift into the ring and a reorientation of the cytosine carbon-6 double bond, i.e., $C = N:_{ring} → C = N:H_{side chain}$, illustrated in Figure 2b. Quantum uncertainty arguments are also consistent with the observation that time-dependent CpG → TpG is ~ 10 to 50-fold greater when cytosine is methylated [185-186]. A consequence of $-CH_3$ attached to cytosine carbon-5 is additional proton-proton interaction for cytosine amino protons, i.e., $-NH_2 - - H_3C-$ [17,163]. This enhances probabilities of quantum uncertainty limits, Δx $\Delta p_x \geq \frac{1}{2}$ ℏ, operating on meta stable amino cytosine protons, causing further proton confinement to too small of space, Δx, thereby increasing proton kinetic energy which would increase probabilities of *keto-amino → enol-imine* arrangements by the asymmetric channel (Figure 2b), consistent with observation [185-186].

In the case of the symmetric channel (Figure 2a), quantum uncertainty limits, Δx $\Delta p_x \geq \frac{1}{2}$ ℏ, initially operate on hydrogen bonding amino ($-NH_2$) protons of carbon–2 guanine, which introduces the initial EPR arrangement, *keto-amino → enol-imine* (Figure 2a) where position – momentum entanglement is introduced between separating enol and imine protons [17,35-39]. Proton departure causes a reorganization of π and σ electrons in guanine. Proton arrival at carbon-2 keto on cytosine induces (a) quantum uncertainty limits, Δx $\Delta p_x \geq \frac{1}{2}$ ℏ, operating on amino ($-NH_2$) protons of carbon-6 cytosine, thereby generating the second EPR arrangement, *keto-amino → enol-imine*, and simultaneously, (b) a reorganization of π and σ electrons, including double bond shifts, $C = N:_{ring} → C = N:H_{side chain}$ at carbon-2 guanine and carbon-6 cytosine, illustrated in Figure 2a.

Entangled proton qubit states at $G'-C'$, $*G-*C$ and $*A-*T$ sites are introduced as consequences of EPR arrangements, *keto-amino → enol-imine*, via symmetric and asymmetric channels (Figure 2-4), where product enol and imine protons are shared between two different sets of indistinguishable electron lone pairs. Consequently, product protons participate in entangled quantum oscillations at ~ $10^{13}s^{-1}$ through intervening barriers between near symmetric double minima in decoherence-free subspaces [54,67-69] until "measured by" [35-40] an enzyme quantum reader. In addition to satisfying bizarre (via classical standards) molecular genetics transcription and replication observables [15-17,20-21,27], this model agrees with the basic tenets of quantum information theory [35-45], and further, provides insight into ancestral mechanisms responsible for primordial pool RNA [57-61] and DNA [4,28,35-36] genomic evolution in terms of ribozyme – proton, and enzyme – proton, entanglement processing [37-39].

Metastable hydrogen bonding amino ($-NH_2$) protons encounter quantum uncertainty limits, Δx $\Delta p_x \geq \frac{1}{2}$ ℏ, which generate probabilities of EPR arrangements, *keto-amino → enol-imine*, where position – momentum entanglement is

introduced between separating product protons. The symmetric channel (Figure 2a) is initiated by reactive protons originating on amino (–NH$_2$) carbon-2 guanine, whereas the asymmetric channel (Figure 2b) is a consequence of reactive protons emerging from amino (–NH$_2$) carbon-6 cytosine. The "sequence of events" for generating distinguishable sets of entangled proton qubits exhibited as heteroduplex heterozygote isomer pairs, G-C → *G′-C′* and G-C → **G-*C* [23], is based on observation [15-16,20-21] and approximate quantum chemical calculations [17,54], and further, implies a coupling between the motion of the two, or four, reactive amino (–NH$_2$) protons and intramolecular reorganization of π and σ electrons [35-36,165].

Thus, as opposed to a "simultaneous tunneling" of two hydrogen bonded protons at their instantaneous energy levels, observation [20-21,23] and the model [15-17,35-39] are consistent with EPR arrangements, *keto-amino → enol-imine*, generated by an initially energetic amino proton, with the second proton transfer during electron reorganization, which could cause reductions in barrier height for the second proton. This model for exchange tunneling time-dependence can be simulated in terms of a single regular proton and a "composite proton", of mass equal two protons (Appendix I). A discussion of the energetics and dynamics of proton exchange tunneling in terms of "standard" G-C is given by Zoete and Meuwly [187], where EPR-generated entangled proton qubits [35-39] are neglected.

Based on the present report, accurate treatments for *in vivo* origination of *G′-C′* and **G-*C heteroduplex heterozygote* superposition sites [15-17,20-21,38] should account for experimentally observable consequence of quantum uncertainty limits, Δx Δp$_x$ ≥ $\hbar$/2, operating on metastable hydrogen bonding amino protons [35-39]. This causes direct quantum mechanical proton – proton physical interaction in a confined space, Δx [2,66], which generates probabilities of EPR arrangements [29-31], *keto-amino → enol-imine*, exhibited as heteroduplex heterozygotes, G-C → *G′-C′* and G-C → **G-*C* [23,35-39,54]. Reduced energy product enol and imine proton qubits occupy intramolecular decoherence-free subspaces [11,67-69] between indistinguishable sets of electron lone-pairs, and consequently, participate in entangled quantum oscillations at ~10^{13} s^{-1}between near symmetric energy wells until measured, in a genome groove (~ 22 Å or 12 Å [70]), δt << 10^{-13} s, by an enzyme Grover's-type quantum processor [35-40].

The resulting enzyme – proton entanglement implements quantum information processing [40-45], Δt′ ≤ 10^{-14} s [13], instructions before proton decoherence [14]. The decohered state is then biologically processed, yielding observables, e.g., *ts* and *td* [15-17,35-39]. Credible molecular models, with accurate boundary conditions for *in vivo* duplex DNA G-C "ground state" configure rations (Appendix I), cannot neglect participation of EPR-generated entangled proton qubits creating time-dependent heteroduplex heterozygote *G′-C′* and **G-*C* super positions [15-17,20-21], that are subsequently "measured by" Grover's-type [35-40] enzyme quantum processors, which implement quantum information processing, Δt́ ≤ 10^{-14} s, to yield molecular clock, *ts* and *td* [15-17,23,35-39,49-50,54,100].

Approximate Lifetimes of Metastable keto-amino Protons

Recent studies [16-17,35-39] imply replicase systems [28] create a DNA double helix containing metastable amino (–NH$_2$) hydrogen bonding protons [65] that satisfy the criteria for a non-interacting isolated system [12], which is not at equilibrium since reduced energy enol and imine proton qubit states are energetically accessible, but initially unoccupied. Consequently, quantum uncertainty limits, Δx Δp$_x$ ≥ $\hbar$/2, operate on meta stable hydrogen bonding amino (–NH$_2$) protons which generate probabilities of EPR arrangements, *keto-amino → enol-imine,* illustrated in Figure 1-4 [15-17,20-23,35-39]. These EPR-generated entangled proton qubits imply energy conservation along reactant and product coordinates [133] and intramolecular charge conservation, thereby avoiding energetically unstable ionic states. Since unperturbed, reduced energy enol and imine entangled proton qubit states will not repopulate the original meta stable keto-amino state, an approximate relationship between the characteristic lifetime, τ, of the meta stable state and the total transition rate, Γ, out of the unstable state can be expressed as [2]

$$\Gamma = \sum_{f} W_{if} = 1/\tau \quad (40)$$

where W$_{if}$ is the transition rate out of the unstable state and the sum Σ$_f$ is over all final enol and imine states. Based on experimental measurements, order of magnitude estimates are listed in Table 5 for *ts* events per G-C (and *td* events per A-T) at 37 ^{0}C. Equation (40) is solved for τ to yield the mean lifetime of metastable protons for each Γ value in Table 5.

The value, Γ = 9.76×10⁻¹² ts/GC/s, is obtained from the study by Baltz et al. [20] where forward, $r_+ \rightarrow r$, ts rates were measured as a function of temperature in T4 phage. Kricker and Drake [24] reported a 37 °C ts transversion rate of 4×10⁻⁹ events per G-C per hr, which is 9.6×10⁻⁸ per 24 hr. However, a value of 1.92×10⁻⁷ per 24 hr (=2×9.6×10⁻⁸) would include both time-dependent transversions and transitions since their average rates are approximately equal [20,21]. This yields a Γ value of 2.22×10⁻¹² s⁻¹, listed in Table 5. Drake and Baltz [22] have estimated ts/GC/day to be ~ 4×10⁻⁸ or 4.63×10⁻¹³ts/GC/s at 37 °C. The Γ value for time-dependent deletions at *A-*T sites is, Γ = 5.32×10⁻¹²td/AT/s [16], which is in order of magnitude agreement with two of the three values in Table 5. Data yielding Γ values in Table 5 include experimental contributions from both symmetric and asymmetric channels (Figure 2 & 3) for populating entangled proton qubit states at G'-C', *G-*C and *A-*T sites. In this order of magnitude treatment, no distinction is made between the symmetric and asymmetric channels for generating reduced energy, entangled proton qubit states.

<k> (events/24 hrs)	Γ (sec-1)	τ (yrs)
8.43×10-7	9.76×10-12	3246
1.92×10-7	2.22×10-12	14273
4×10-8	4.63×10-13	68436
†4.60×10-7	5.32×10-12	5956

†Deletions at *A-*T sites

Table 5: Relationship between events per G-C or A-T per 24 hrs, <k>, events per sec, Γ, and mean lifetimes, τ, of meta stable keto-amino Hydrogen-bonding protons.

It is instructive to compare measurements (estimates) of mutation events per bp per unit time for T4 phage (Table 5) and the human genome. For example, Nachman and Crowell [184] obtained a value of ~ 2.5×10⁻⁸ mutations per bp per generation for the human diploid genome. If the cell generation time is two weeks (336 hr), the events per bp per year are 6.52×10⁻⁶. The T4 phage rate of 8.43×10⁻⁷ (events/24 hr) yields a value of 3.1×10⁻⁴ events/GC/yr. The replacement of cytosine with 5HMC in T4 phage DNA causes further proton confinement to too small of space, Δx, thereby enhancing reaction rates, G-C → *G-*C (Figure 2) by ~ 10- to 50-fold [163,185-186]. The ratio, (3.1×10⁻⁴)/(6.52×10⁻⁶) = 47.5, implies "ballpark" agreement between T4 phage DNA rates, containing 5HMC, and mutation rates for regular human DNA. However, T4 phage mutations were introduced, exclusively, by EPR-generated entangled proton qubits, yielding **ts** and **td,** whereas all EPR and classical modes of mutation contributed to the human mutation spectrum [71,188].

To include mass effects in exchange tunneling of two protons, the present treatment evaluates exchange tunneling time-dependence in terms of a regular proton, of mass m = 1.67252×10⁻²⁴ g, and a composite proton of mass m = 3.34×10⁻²⁴ g. Accordingly at t = 0, the regular proton is in the meta stable energy well, illustrated in Figure 1, which is separated from the deeper enol-imine energy well by a parabolic barrier of height V_0 = (V– E) eV and width a_o angstroms (Å). The characteristic lifetime, τ, of the meta stable proton in an initial energy well can be estimated in terms of the Gurney and Condon [189] approximation given by

$$\tau \approx r_o (m/2E)^{1/2} \exp\{a_o \pi /2\hbar[2m(V-E)]^{1/2}\}, \quad (41)$$

where r_o = 0.6 Å, width of the classical energy well, and m = 1.67252×10⁻²⁴ g, mass of the regular proton.

Since interstrand hydrogen bonded keto-amino protons in duplex DNA oscillate at frequencies the order of 10¹³ to 10¹⁴ s⁻¹, this report uses ν = 5×10¹³ s⁻¹ as the frequency [161]. Ground level keto-amino proton energy is E = hν = 0.206 eV where Planck's constant h is 6.625×10⁻²⁷ erg-sec. Equation (41) can be rewritten as

$$\tau = 0.95 \times 10^{-14+14.976a_o\sqrt{V_o}} \quad (42)$$

where (V – E) is defined as V_0 in units of eV. Equation (42) is used to calculate lifetimes, τ, of meta stable protons in Table 6. Here potential energy barrier heights, V_0, vary from 4.25 to 5.25 eV in increments of 0.25 eV, and tunneling distances, a_o, vary from 0.74 to 0.800 Å in increments of 0.010 Å. This range of a_o and V_0 values is selected to be compatible with dimensions of DNA hydrogen bonds [187] and generate metastable proton lifetimes, τ, that approximate experimentally determined values in Table 5, i.e., ~ 3200, ~ 6000, ~ 14000 and ~ 68000 yrs. Calculations in

Table 6 indicate lifetimes of $\sim$ 3200 yrs could be expected for a_o and V_0 values along the line from $a_o \approx 0.788$Å with $V_0 = 4.5$eV to $a_o \approx 0.746$Å with $V_0 = 5.0$eV. Lines of approximately constant τ in Table 6 are shown for τ = 3200, 6000, 14000 and 68000 yrs.

a_o (Å)	τ (yrs) V_0 (4.25 eV)	τ (yrs) V_0 (4.50 eV)	τ (yrs) V_0 (4.75 eV)	τ (yrs) V_0 (5.00 eV)	τ (yrs) V_0 (5.25 eV)
0.74	21	97	428	1817	7433
0.75	43	202	908	3927	16381
0.76	88	420	1926	8491	36097
0.77	178	872	4083	18359	79546
0.78	363	1813	8657	39697	175292
0.79	739	3767	18354	85822	386282
0.80	1505	7829	38917	185554	851232

Table 6: Mean lifetimes, τ (yrs), of a Meta stable regular proton (m = 1.67252×10^{-24} g) before encountering quantum uncertainty limits, $\Delta x \Delta p_x \geq \hbar/2$, and penetrating potential energy barrier heights.
(Table 6 Mean lifetimes, τ (yrs), of a meta stable regular proton (m = 1.67252×10^{-24} g) before penetrating potential energy barrier heights, V_0 (eV), of 4.25, 4.50, 4.75, 5.00 and 5.25 eV where the one dimensional tunneling distance, a_o (Å) is varied from 0.74 to 0.8 Å in increments of 0.01 Å. Mean lifetime calculations use Eq (42) where proton frequency is $\nu = 5 \times 10^{13}$ s^{-1}. Approximate lines of constant τ are indicated for τ = 3200, 6000, 14000, 68000 yrs.)

For purposes of including mass effects on time-dependence of generating entangled proton qubits, the regular proton is replaced by a composite proton, of mass m = 2 protons (3.34×10^{-24} g). The corresponding form of Eq (42) is rewritten as

$$\tau = 1.35 \times 10^{-14 + 21.179 a_o \sqrt{V_o}} \quad (43)$$

where (V – E) is defined as V_0 in units of eV. Equation (43) is used to calculate lifetimes of meta stable composite protons in Table 7. Here potential energy barrier heights, V_0, vary from 2.10 to 2.60 eV, and tunneling distances, a_o, vary from 0.700 to 0.800 Å in increments of 0.010 Å. This range of a_o and V_0 values is selected to be compatible with dimensions of hydrogen bonds and generate meta stable proton lifetimes, τ, that approximate experimentally determined values in Table 5. Calculations in Table 7 indicate lifetimes of $\sim$ 3200 yrs could be expected for a_o and V_0 values along the line from $a_o \approx 0.784$Å with $V_0 = 2.25$ eV to $a_o \approx 0.727$Å with $V_0 = 2.6$ eV. Lines of constant τ are identified in Table 7 for τ = 3200, 6000, 14000, and 68000 yrs.

a$_o$ (Å)	τ (yrs) V_0 (2.10 eV)	τ (yrs) V_0 (2.25 eV)	τ (yrs) V_0 (2.35 eV)	τ (yrs) V_0 (2.50 eV)	τ (yrs) V_0 (2.60 eV)
0.70	1	7	23	118	344
0.71	3	15	48	255	755
0.72	5	32	102	552	1657
0.73	11	66	215	1193	3637
0.74	22	138	454	2579	7985
0.75	45	287	958	5577	17530
0.76	90	596	2023	12058	38484
0.77	183	1239	4272	26070	84486
0.78	372	2574	9022	56365	185474
0.79	754	5349	19053	121865	407178
0.80	1528	11117	40237	263480	893894

(Lines of constant τ shown approximately for τ = 3200, 6000, 14000, 68000 yrs.)

Table 7: Mean lifetimes, τ (yrs), of a meta stable composite proton (m = 3.34×10^{-24} g) before penetrating potential energy barrier heights.

(Table 7 Mean lifetimes, τ (yrs), of a meta stable composite proton (m = 3.34×10^{-24} g) before penetrating potential energy barrier heights, V$_0$ (eV), of 2.10, 2.25, 2.35, 2.50 and 2.60 eV where the one dimensional tunneling distance, a$_o$ (Å) is varied from 0.70 to 0.8 Å in increments of 0.01 Å. Mean lifetime calculations use Equation (43) where composite proton frequency is ν = 5×10^{13} s^{-1}. Lines of constant τ are shown, approximately, for τ = 3200, 6000, 14000, 68000 yrs.)

Model Calculations for Proton Qubit Oscillations, Using a Double Minimum Symmetric Potential and an Asymmetric Double Minimum Potential

Energy surfaces "seen by" enol and imine protons are near symmetric since significant components are contributed by two intramolecular sets of indistinguishable electron lone-pairs located on each enol and imine hydrogen-bond end group. In these cases, enol and imine protons will participate in entangled quantum oscillation through intervening barriers between near symmetric double-minima [17,54]. Order of magnitude estimates of quantum oscillation frequencies use both a regular proton (m = 1.67252×10^{-24} g) and the composite proton (m = 3.34×10^{-24} g) on a one-dimensional model, double-minimum symmetric energy surface illustrated in Figure 20.

An estimate for the interminimal distance, θ, can be given by specifying distances identified in Figure 1. The distance L between the enol O and imine N is taken as L = 2.8775 Å for the symmetric channel (Figure 2a) and L = 2.9135 Å for the asymmetric channel (Figure 2b). These values are obtained from an average of the reactant state G-C distances given by Zote and Meuwly [187], i.e., from their Figure 1, (2.901 + 2.854)/2 = 2.8775 Å and (2.854 + 2.973)/2 = 2.9135 Å. The central energy barrier, a$_o$, is initially assigned a width of 0.775 Å with r$_o$ = 0.6 Å.

From these approximate dimensions, interminimal distances, θ in Figure 20, can be estimated by defining ℓ as ℓ = L – (r$_o$ + r$_o$ + a$_o$) so that θ is given by θ^2 = (ℓ/2)^2 + (ℓ/2)^2, illustrated in Figure 21. For the symmetric channel, one obtains ℓ_s = 2.8775 – (0.6 + 0.6 + 0.775) = 0.9025 Å and the expression for the asymmetric channel is ℓ_a = 2.9135 – (0.6 + 0.6 + 0.775) = 0.9385 Å. The corresponding θ relations are $_s$θ^2 = (0.9025/2)^2 + (0.9025/2)^2 and $_a$θ^2 = (0.9385/2)^2 + (0.9385/2)^2, yielding θ$_s$ = 0.6382 Å (Table 8a) and θ$_a$ = 0.6636 Å (Table 8b). Additional a$_o$ values (Figure 1) of a$_o$ = 0.750 Å and a$_o$ = 0.725 Å are considered, yielding corresponding θ values of θ$_s$ = 0.6558 Å & θ$_s$ = 0.6736 Å (Table 8a) and θ$_a$ = 0.6813 Å & θ$_a$ = 0.6990 Å (Table 8b). The interminimal tunneling barrier, ϕ_o (Figure 20), is given by ϕ_o = θ – (η/2 + η/2) where, in the symmetric double well, the classically allowed energy wells, η, are parabolic of width 0.6 Å. The intervening

energy barriers, ϕ_o, for the symmetric channel are $_s\phi_o$= 0.0382, 0.0558, 0.0736 Å (Table 8a) and for the asymmetric channel, $_a\phi_o$ = 0.0636, 0.0813, 0.0990 Å, listed in Table 8b.
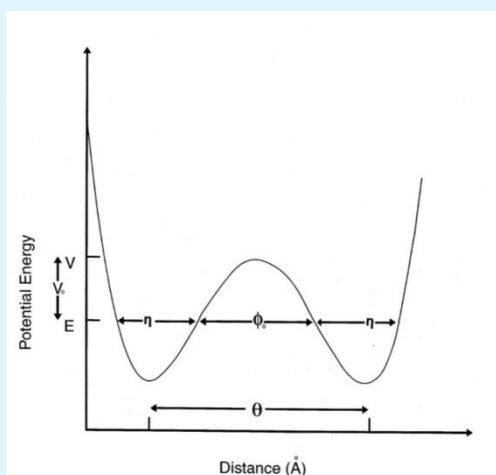

Figure 20: Double minimum symmetric potential energy surface.
(Figure 20 Double minimum symmetric potential energy surface for regular and composite enol and imine entangled proton qubits.)

The proton frequency along the θ-axis is taken as ν = 5×10^{13} s^{-1}. On the symmetric energy surface of Figure 20, the time interval for the proton in either energy well is equal. Thus, the escape time, τ, from the left well equals that from the right well; so, proton qubit oscillation frequencies in Table 8-9 are given by $\nu_\theta = 1/2\tau$. Escape times, τ, for regular protons use Eq (42) for qubit frequency calculations, ν_θ, listed in Table 8. Potential energy barrier heights, ν_o, vary from 0.10 eV to 0.30 eV in increments of 0.05 eV and proton qubit oscillation frequencies, ν_θ, vary from 8.11×10^{12} to 3.47×10^{13} s^{-1} for regular protons in Table 8.

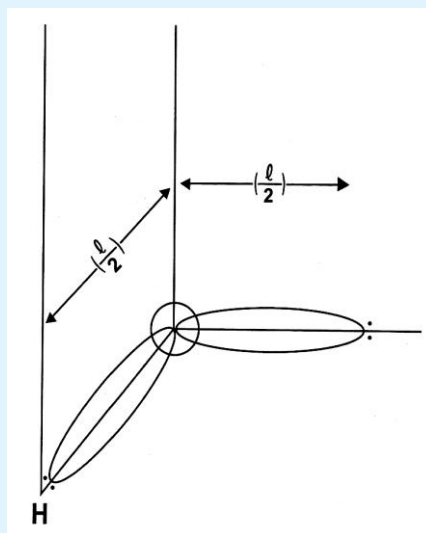Figure 21: Schematic representation of dimensions for determining the interminimal qubit distance, θ (listed in Table 8-9 for enol and imine entangled proton qubits.)

Similar qubit oscillation frequency calculations for composite protons in "asymmetric" energy wells are listed in Table 9, using Eq (43). In this case, proton qubit oscillation frequencies vary from 2.63×10^{12} to 2.05×10^{13} s^{-1}.

φ_o (Å)	θ (Å)	ν_θ (s^{-1}) V_0 (0.10 eV)	ν_θ (s^{-1}) V_0 (0.15 eV)	ν_θ (s^{-1}) V_0 (0.20 eV)	ν_θ (s^{-1}) V_0 (0.25 eV)	ν_θ (s^{-1}) V_0 (0.30 eV)
(a)						
0.0382	0.6382	3.47×10^{13}	3.16×10^{13}	2.92×10^{13}	2.72×10^{13}	2.56×10^{13}
0.0558	0.6558	2.86×10^{13}	2.50×10^{13}	2.23×10^{13}	2.01×10^{13}	1.83×10^{13}
0.0736	0.6736	2.36×10^{13}	1.97×10^{13}	1.69×10^{13}	1.48×10^{13}	1.31×10^{13}
(b)						
0.0636	0.6636	2.63×10^{13}	2.25×10^{13}	1.97×10^{13}	1.76×10^{13}	1.58×10^{13}
0.0813	0.6813	2.17×10^{13}	1.78×10^{13}	1.50×10^{13}	1.30×10^{13}	1.13×10^{13}
0.0990	0.6990	1.79×10^{13}	1.40×10^{13}	1.14×10^{13}	9.55×10^{12}	8.11×10^{12}

Table 8: "Flip-flop" frequencies, ν_θ (s^{-1}), for regular enol and imine entangled proton qubits – oscillating between symmetric energy wells, Figure 20
(Table 8 "Flip-flop" frequencies, ν_θ (s^{-1}), for regular enol and imine entangled proton qubits – oscillating in symmetric energy wells at a frequency $\nu = 5\times10^{13}$ s^{-1} – to tunnel back and forth between the symmetric double minimum potential illustrated in Figure 20. Energy barriers, V_0, vary from 0.10 to 0.30 eV in increments of 0.05 eV, and the one-dimensional tunneling distance, ϕ_o, varies from (a) 0.0382 to 0.0736 Å for the symmetric channel (Figure 2-3) and (b) from 0.0636 to 0.0990 Å for the asymmetric channel. Interminimal distances, θ, vary from (a) 0.6382 to 0.6736 Å for the symmetric channel and from (b) 0.6636 to 0.6990 Å for the asymmetric channel.)

To simulate tunneling frequencies of a regular proton on a near symmetric energy surface, V_0 (eV) and ϕ_o (Å) values in Table 8 are each reduced by 20% for one of the two energy wells displayed in Figure 20. The resulting qubit oscillation frequency calculations are shown in Table 10 where the asymmetric energy barriers are designated by v/V_0 (e.g., 0.08/0.1 in 2nd column) and a symmetric tunneling distance are identified by ϕ/Φ_o, e.g., 0.0306/0.0382 in the first row.

Since the symmetric surface of Figure 20 (calculations in Table 8) was rendered asymmetric by reducing both V_0 and ϕ_o by 20% each, the proton will spend less time in the shallower energy well with a reduced classical barrier.

φ_o (Å)	θ (Å)	ν_θ (s^{-1}) V_0 (0.10 eV)	ν_θ (s^{-1}) V_0 (0.15 eV)	ν_θ (s^{-1}) V_0 (0.20 eV)	ν_θ (s^{-1}) V_0 (0.25 eV)	ν_θ (s^{-1}) V_0 (0.30 eV)
(a)						
0.0382	0.6382	2.05×10^{13}	1.80×10^{13}	1.61×10^{13}	1.46×10^{13}	1.34×10^{13}
0.0558	0.6558	1.57×10^{13}	1.29×10^{13}	1.10×10^{13}	9.50×10^{12}	8.34×10^{12}
0.0736	0.6736	1.19×10^{13}	9.22×10^{12}	7.44×10^{12}	6.16×10^{12}	5.19×10^{12}
(b)						
0.0636	0.6636	1.36×10^{13}	1.11×10^{13}	9.25×10^{12}	7.85×10^{12}	6.77×10^{12}
0.0813	0.6813	1.06×10^{13}	7.98×10^{12}	6.29×10^{12}	5.10×10^{12}	4.22×10^{12}
0.099	0.699	8.05×10^{12}	5.71×10^{12}	4.28×10^{12}	3.31×10^{12}	2.63×10^{12}

Table 9: Flip-flop frequencies, ν_θ (s^{-1}), for the composite enol and imine entangled proton qubit, oscillating between its classically allowed, symmetric energy wells, Figure 20.

Consequently, compared to the symmetric surface (Table 8), quantum oscillation frequencies on this asymmetric surface will be slightly enhanced as illustrated in Table 10. Here the frequency, ν_θ, is calculated from $\nu_\theta = 1/(\tau + \tau_{0.8})$ where $\tau_{0.8}$ is the escape time from the shallow energy well and the calculated frequency range is from 1.02×10^{13} to 3.68×10^{13} s^{-1}. A similar consideration of the composite proton on this asymmetric energy surface uses Equation (43) to calculate qubit oscillation frequencies, given by $\nu_\theta = 1/(\tau + \tau_{0.8})$, and listed in Table 11. Here the frequency range for the composite proton is from 3.83×10^{12} to 2.23×10^{13} s^{-1}.

ϕ/Φ_0 (Å)	ν_θ (s^{-1}) v/V$_0$ (0.08/0.1)	ν_θ (s^{-1}) v/V$_0$ (0.12/0.15)	ν_θ (s^{-1}) v/V$_0$ (0.16/0.20)	ν_θ (s^{-1}) v/V$_0$ (0.20/0.25)	ν_θ (s^{-1}) v/V$_0$ (0.24/0.30)
(a)					
0.0306/0.0382	3.68×10^{13}	3.39×10^{13}	3.16×10^{13}	2.98×10^{13}	2.82×10^{13}
0.0446/0.0558	3.11×10^{13}	2.76×10^{13}	2.50×10^{13}	2.29×10^{13}	2.11×10^{13}
0.0589/0.0736	2.63×10^{13}	2.24×10^{13}	1.96×10^{13}	1.74×10^{13}	1.57×10^{13}
(b)					
0.0509/0.0636	2.89×10^{13}	2.52×10^{13}	2.25×10^{13}	2.03×10^{13}	1.85×10^{13}
0.0650/0.0831	2.44×10^{13}	2.05×10^{13}	1.77×10^{13}	1.55×10^{13}	1.38×10^{13}
0.0792/0.0990	2.06×10^{13}	1.66×10^{13}	1.34×10^{13}	1.18×10^{13}	1.02×10^{13}

Table 10: Flip-flop frequencies, ν_θ (s^{-1}), for regular enol and imine entangled proton qubits, on an asymmetric energy surface

(Table 10 Flip-flop frequencies, ν_θ (s^{-1}), for regular enol and imine entangled proton qubits of Table 8 to tunnel back and forth between near symmetric double minimum potentials. In this case, the one dimensional tunneling distance, ϕ_0 (Å), and the energy barrier, V_0 (eV), are each reduced by 20% for the left-hand well. This is indicated by ratios, ϕ/Φ_0 (e.g., 0.0306/0.0382) for tunneling distances and v/V$_0$ (e.g. 0.08/0.1) for energy barriers.)

Enhanced stability of enol and imine entangled proton qubits can be estimated by including quantum effects of proton qubit oscillations. This quantum mixing of proton energy states introduces the quantum mechanical energy splitting term, Ω, such that the average energy, E_0, is split by $\pm\,\Omega$. In the approximation that each enol and imine proton would contribute $E_0 - \Omega$ to the energy, stability enhancements can be estimated by $2\Omega = h\nu_\theta$ where h is Planck's constant and ν_θ is the quantum oscillation frequency. Quantum oscillation frequency calculations for regular protons (Tables 8, 10) and for composite protons (Table 9, 11) identify a frequency range of 2.63×10^{12} to 3.68×10^{13} s^{-1}. Duplex states with four entangled proton qubits would be stabilized by 4Ω, whereas reduced energy states with only two proton qubits would be stabilized by 2Ω. Protons exhibiting quantum oscillation frequencies listed in Table 9 would emit infrared and stability enhancements would vary, approximately, from 0.25 to 7.15 Kcal/mole.

ϕ/Φ_0 (Å)	ν_θ (s^{-1}) v/V$_0$ (0.08/0.1)	v/V$_0$ (0.12/0.15)	ν_θ (s^{-1}) v/V$_0$ (0.16/0.20)	ν_θ (s^{-1}) v/V$_0$ (0.20/0.25)	ν_θ (s^{-1}) v/V$_0$ (0.24/0.30)
(a)					
0.0306/0.0382	2.23×10^{13}	2.02×10^{13}	1.84×10^{13}	1.69×10^{13}	1.57×10^{13}
0.0446/0.0558	1.76×10^{13}	1.51×10^{13}	1.31×10^{13}	1.16×10^{13}	1.04×10^{13}
0.0589/0.0736	1.38×10^{13}	1.05×10^{13}	8.57×10^{12}	7.17×10^{12}	6.10×10^{12}
(b)					
0.0509/0.0636	1.58×10^{13}	1.36×10^{13}	1.16×10^{13}	1.01×10^{13}	8.93×10^{12}
0.0650/0.0831	1.24×10^{13}	1.01×10^{13}	8.26×10^{12}	6.90×10^{12}	5.86×10^{12}
0.0792/0.0990	9.77×10^{12}	7.53×10^{12}	5.86×10^{12}	4.69×10^{12}	3.83×10^{12}

Table 11: Flip-flop frequencies, ν_θ (s^{-1}), for the composite enol and imine entangled proton qubit, on an asymmetric surface.

(Table 11: Flip-flop frequencies, ν_θ (s^{-1}), for the composite enol and imine entangled proton qubit of Table 9 to tunnel back and forth between a near symmetric double minimum potential. Energy surface parameters are identical to those for the regular proton given in Table 10.)

Qualitative Estimates for Proton Decoherence Times

Quantum informational content within entangled proton qubit states occupying a *G′-C′* or **G-*C* site (Figure 2-3) is deciphered and processed by a Grover's-type enzyme – proton entanglement to yield *ts* and *td*. In intervals, $\delta t \ll 10^{-13}$ s, the enzyme quantum reader "measures" quantum informational content embodied within an entangled proton qubit "captured" in a DNA groove [70].

ν_θ (10^{13} s^{-1})	2Ω (Kcal/mole)	4Ω (Kcal/mole)
3.7	3.56	7.15
3.5	3.38	6.76
3	2.9	5.8
2.2	2.16	4.25
1.5	1.45	2.9
0.93	0.9	1.8
0.43	0.42	0.84
0.26	0.25	0.5

Table 12: Stability enhancements (Kcal/mole) for duplex enol and imine entangled proton states calculated from $\Delta E = h\nu_\theta = 2\Omega$ for flip-flop frequencies, ν_θ, in the range of 2.6×10^{12} to 3.7×10^{13} s^{-1}. Each enol-imine hydrogen bond is assumed to provide an enhancement of 2Ω.

An observable information output from transcription of entangled qubits [16-17,38] is immediately generated [20-23], e.g., *G'2 0 2 → T2^2 0 2^2*. This quantum transcription measurement introduces an entanglement between the coherent groove proton(s) and proximal enzyme components which, in intervals, $\Delta t' \leq 10^{-14}$ s, implements and completes a quantum search algorithm to create the requisite complementary mispair (e.g., Figure 6) for the particular *ts* or *td* [15-17,20-21,35-39,54]. The entangled enzyme-proton complex retains quantum coherence until the complementary mispair is specified (see Table 2).

The time scale over which quantum coherence is lost by superposition proton qubit states in duplex DNA can be estimated in terms of the treatment by Zurek [190]. Accordingly, off-diagonal terms in the density matrix will decay at a rate τ_D^{-1} where decoherence time, τ_D, is given, approximately, by

$$\tau_D \approx \gamma^{-1}\left(\lambda_T / \Delta X^2\right) \quad (45)$$

Here λ_T is the thermal de Broglie wave length for a quantum proton with two degrees of freedom and Δx is the interminimal distance, θ, displayed in Figure 20. A relaxation time, $\tau_R = \gamma^{-1}$, is the time for energy dissipation between coherent states and is a measure of the speed of energy dissipation due to a coherent proton interacting with its immediate environment. The thermal de Broglie wavelength for a single proton is $\lambda_T = \hbar/(2mkT)^{1/2} = 4.91/(T)^{1/2} = 0.28$ Å for T= 310 K, 37^0 C. In the case of a composite proton, $\lambda_T = 0.197$ Å, whereas if m is mass of four protons, $\lambda_T = 0.139$ Å. EPR-generated proton qubits shared between two indistinguishable sets of electron lone-pairs in duplex DNA [35-39] can occupy decoherence-free subspaces [67-69], and through certain degrees of freedom [11,13,99], may avoid decoherence until "processed by" the enzyme quantum reader [35-40]. After initiation of enzyme – proton entanglement processing, Equation (45) allows an estimate of the ratio, $\tau_D/\tau_R = (\lambda_T/\Delta x)^2$, which is given in Table 12 for mass m = 1 proton, 2 protons and 4 protons. Consistent with Table 8-9, the interminimal distance, Δx (θ of Figure 20), is varied from 0.5 to 0.7 Å. The first entry in Table 13, $\Delta x = 0.5$ Å, indicates that a quantum proton would remain coherent for $\sim$ 30% of the relaxation time, τ_R, i.e., $\tau_D/\tau_R = 0.31$. In the case of a composite proton where $\Delta x = 0.5$ Å, $\tau_D/\tau_R = 0.16$; so, the composite proton would maintain quantum coherence for about 16% of the relaxation time. The bottom row in Table 13 gives the corresponding τ_D/τ_R ratios when the mass m = 4 protons.

No. Protons	τ_D/τ_R	τ_D/τ_R	τ_D/τ_R	τ_D/τ_R	τ_D/τ_R	τ_D/τ_R
	Δx	Δx	Δx	Δx	Δx	Δx
	0.5	0.55	0.6	0.64	0.68	0.7
1	0.31	0.26	0.22	0.19	0.17	0.16
2	0.16	0.13	0.11	0.1	0.09	0.08
4	0.08	0.06	0.05	0.05	0.04	0.04

Table 13: Ratios, $\tau_D/\tau_R = (\lambda_T/\Delta x)^2$, where Δx (Å) is varied from 0.5 to 0.7 Å and mass m, in $\lambda_T = \hbar/(2mkT)^{1/2}$, equals 1, 2 and 4 protons.

Proton qubit oscillation frequency calculations (Table 8-9) imply the enzyme quantum reader must implement its genetic specificity reading of an entangled proton qubit, H^+, occupying a DNA groove [11,28,70] in intervals, $\delta t \ll 10^{-13}$ s [13]. This quantum measurement on an entangled proton qubit determines, instantaneously, microphysical specifications for implementing entangled enzyme quantum searches, $\Delta t' \leq 10^{-14}$ s, that specify the selected *ts* for the "measured" superposition, $G'\text{-}C'$ or $*G\text{-}*C$ states (Figure 2-3). According to Table 13, a quantum proton would retain coherence for about 16 to 30% of the relaxation time, τ_R. Evidently, this approximately 16 to 30% availability of τ_R is sufficient time for the enzyme – proton entanglement complex to (*i*) implement its initial measurement on an entangled qubit, H^+, "trapped" in a DNA groove and (*ii*) complete its entangled enzyme-proton quantum search specification of the complementary mispair (Figure 6), and execute quantum information processing before proton decoherence [13-14]. Since $\delta t \ll 10^{-13}$ s and $\Delta t' \leq 10^{-14}$ s, an order of magnitude estimate of decoherence time can be given as $\Delta t' < \delta t < \tau_D \leq 10^{-13}$ s. This "ballpark" estimate is in order of magnitude agreement with Tegmark's [13] more rigorous calculations.